

Northumbria Research Link

Citation: McHale, Glen, Brown, Carl, Newton, Michael, Wells, Gary and Sampara, Naresh (2011) Dielectrowetting Driven Spreading of Droplets. *Physical Review Letters*, 107 (18). pp. 186101-186105. ISSN 0031-9007

Published by: American Physical Society

URL: <http://dx.doi.org/10.1103/PhysRevLett.107.186101>
<<http://dx.doi.org/10.1103/PhysRevLett.107.186101>>

This version was downloaded from Northumbria Research Link:
<http://nrl.northumbria.ac.uk/5205/>

Northumbria University has developed Northumbria Research Link (NRL) to enable users to access the University's research output. Copyright © and moral rights for items on NRL are retained by the individual author(s) and/or other copyright owners. Single copies of full items can be reproduced, displayed or performed, and given to third parties in any format or medium for personal research or study, educational, or not-for-profit purposes without prior permission or charge, provided the authors, title and full bibliographic details are given, as well as a hyperlink and/or URL to the original metadata page. The content must not be changed in any way. Full items must not be sold commercially in any format or medium without formal permission of the copyright holder. The full policy is available online: <http://nrl.northumbria.ac.uk/policies.html>

This document may differ from the final, published version of the research and has been made available online in accordance with publisher policies. To read and/or cite from the published version of the research, please visit the publisher's website (a subscription may be required.)

www.northumbria.ac.uk/nrl



Postprint Version

G. McHale, C.V. Brown, M.I. Newton, G.G. Wells and N. Sampara, *Dielectrowetting driven spreading of droplets*, *Physical Review Letters* **107** (18) (2011) art. 186101; DOI: 10.1103/PhysRevLett.107.186101. The following article appeared in [Physical Review Letters](http://link.aps.org/doi/10.1103/PhysRevLett.107.186101) and may be found at <http://link.aps.org/doi/10.1103/PhysRevLett.107.186101>.

This article may be downloaded for personal use only. Any other use requires prior permission of the author and the American Physical Society. Copyright ©2011 American Physical Society.

Dielectrowetting Driven Spreading of Droplets

G. McHale*, C.V. Brown, M.I. Newton, G.G. Wells, N. Sampara

*School of Science and Technology, Nottingham Trent University
Clifton Lane, Nottingham NG11 8NS, UK*

Abstract

The wetting of solid surfaces can be modified by altering the surface free energy balance between the solid, liquid and vapour phases. Here we show that liquid dielectrophoresis (L-DEP) induced by non-uniform electric fields can be used to enhance and control the wetting of dielectric liquids. In the limit of thick droplets, we show theoretically that the cosine of the contact angle follows a simple voltage squared relationship analogous to that found for electrowetting-on-dielectric (EWOD). Experimental observations confirm this predicted dielectrowetting behavior and show that the induced wetting is reversible. Our findings provide a non-contact electrical actuation process for meniscus and droplet control.

Keywords: Wetting, dielectrophoresis, electrowetting, contact angle, spreading.

PACS Numbers: 68.08.Bc, 68.03.Cd

* To whom correspondence should be addressed. E-mail: glen.mchale@ntu.ac.uk

The wetting of solid surfaces can be modified by changing material or surface properties, such as the surface chemistry or micro- or nano-scale topography,^{1,2} or by introducing additional energies, such as electrostatic.³ This is important for a wide range of processes from microfluidics, whereby large surface area to volume ratios lead to the dominant forces being capillary,⁴ to liquid-based optics, whereby control of the liquid meniscus determines optical properties.^{5,6} In recent years, electrowetting-on-dielectric (EWOD) has been shown to be one of the most versatile and effective methods to actively control the energy balance in the wetting of a solid surface by a droplet.^{3,7,8} In this approach, one or more solid electrodes are coated with a hydrophobic dielectric layer and a droplet of a conducting liquid is then used as the other electrode to create a capacitive structure, but with an electrode contact area dependent on the extent to which the dielectric layer is wetted. This effect modifies the energy balance at the three-phase contact line due to charged ions at the solid-liquid interface, resulting in a contact angle which decreases with applied voltage and which can be used to actuate contact line motion.

Electrowetting has found extensive application in microfluidics⁹ and digitally controlled droplet-based chemical reactions and biological assays,^{10,11} liquid paper,¹² variable focus liquid lenses,^{13,14} to control the Cassie-Baxter to Wenzel transition on superhydrophobic surfaces to create reserve batteries,¹⁵ and to increase coating speeds,¹⁶ to name but a few of its applications. Its functionality has included controlling meniscus curvature, actuating droplet motion, dispensing and mixing liquids and reducing contact angle hysteresis.¹⁷ In general, a liquid subjected to electrostatic fields does not simply show a change in contact angle, but can also experience a strong bulk force.¹⁸ Whilst electrowetting is a versatile method of controlling contact angle, it uses uniform electric fields and requires a conducting liquid in physical contact with an electrode and when operated with a droplet in air often has a high degree of contact angle hysteresis. In this letter, we show that non-uniform electric fields can be used with dielectric liquids and non-contacting electrodes to achieve analogous control of contact angle over a wide range of contact angles and with low degrees of contact angle hysteresis.

The forces on the two charges of a dipole created by polarising a region of material in a uniform electric field balance each other, but when this field is non-uniform, one is larger than the other and an overall force occurs. In a dielectric liquid a non-uniform field therefore causes a bulk force and liquid motion.¹⁹ The use of liquid dielectrophoresis on a circular electrode geometry to create a variable focus lens²⁰ and a microlens array²¹ has been reported, but the theoretical relationship to contact angle and wetting has not been elucidated. To understand how liquid dielectrophoresis might be understood within the context of the wider principles of wetting and control of the contact angle of a droplet, we first consider a uniform layer of a dielectric liquid of depth h on a solid surface with an electric potential that decays with depth of penetration into the liquid, i.e. $V(z)=V_o \exp(-2z/\delta)$, where δ is a penetration depth. The electrostatic energy per unit contact area, w_E , stored in the liquid is then given by integrating the dielectric energy density, $\frac{1}{2}\epsilon_o\epsilon_l \underline{E} \cdot \underline{E}$, where ϵ_l is the dielectric constant of the liquid and $\underline{E}=-\underline{\nabla}V$ is the electric field, over the volume of the liquid in this area,

$$w_E = -\frac{\epsilon_o\epsilon_l V_o^2}{2\delta} \left[e^{-4h/\delta} - 1 \right] \quad (1)$$

In the limit of a liquid layer which is much thicker than the penetration depth of the electric potential the energy per unit contact area of the liquid is $w_E=\epsilon_o\epsilon_l V_o^2/2\delta$. Thus, whilst liquid dielectrophoresis is, in principle, a bulk force, under these conditions it is the change in contact area that causes a change in the net dielectrophoretic force acting upon the liquid. In essence, the

penetration depth of the electric field effectively localizes the effective changes in energy to the vicinity of the solid-liquid interface.

For a droplet, the extent of wetting of a solid surface is given by a local minimum in the surface free energy arising from the solid-vapor, solid-liquid and liquid-vapor interfaces. These are characterized by three interfacial tensions, γ_{SV} , γ_{SL} and γ_{LV} , representing the surface energies per unit area. The effect of increasing the contact area by a small amount, ΔA , is to replace the solid-vapor interface by a solid-liquid interface and so change the surface free energy by $(\gamma_{SL}-\gamma_{SV})\Delta A$. In addition, the movement of the liquid creates an additional liquid-vapor surface area of $\Delta A \cos\theta$ resulting in a surface free energy increase of $\gamma_{LV} \Delta A \cos\theta$.²² In the presence of the non-uniform electric field, and assuming the droplet is sufficiently thick ($h \gg \delta$), there is an additional energy expended of $-\epsilon_o(\epsilon_l-1)V_o^2 \Delta A/2\delta$. For the droplet to be in equilibrium the total change in energy must vanish and so the contact angle adopts a value, $\theta_e(V_o)$, given by,

$$\cos \theta_e(V_o) = \cos \theta_e + \frac{\epsilon_o(\epsilon_l - 1)V_o^2}{2\gamma_{LV} \delta} \quad (2)$$

where Young's law has been used to replace the combination of interfacial tensions by $\cos \theta_e = (\gamma_{SV} - \gamma_{SL})/\gamma_{LV}$. Equation (2) is a liquid dielectrophoresis (L-DEP) modified form of Young's law, which we refer to as "dielectrowetting" in recognition of the effect of L-DEP upon the contact angle. This equation is similar in form to the electrowetting-on-dielectric modified Young's law, but with the ratio of the substrate permittivity to substrate dielectric thickness (ϵ_l/d) replaced by the ratio of liquid permittivity minus that of air to penetration depth $(\epsilon_l-1)/\delta$. It is therefore predicted that an exponentially decaying electric field penetrating into a dielectric liquid will enhance wetting, reducing the contact angle according to equation (2), and so drive a droplet to spread according to magnitude of voltage applied. Formally, eq. (2) predicts that a transition to complete wetting, $\theta_e(V_T)=0$, should occur at a sufficiently high critical voltage, V_T . However, as the droplet spreads and tends to a film its upper liquid-vapor interface comes within the range of the penetration depth. This interface may then change shape, thus providing a mechanism, in addition to the displacement of the three phase contact line, whereby energy may be minimized.^{6,23}

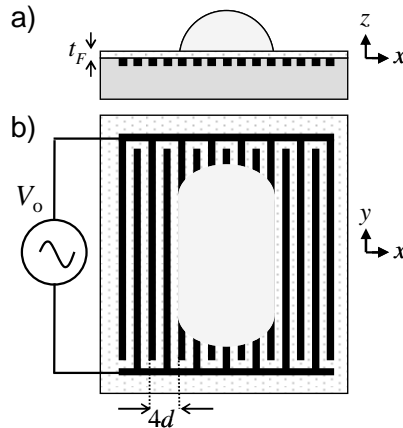


FIG. 1. Schematic of experimental configuration with interdigitated electrode structure with uniform gaps and widths (coated with a thin dielectric layer) generating an exponentially decaying electric field in the vertical direction. Droplet profile viewed (a) parallel to the electrodes, and (b) from above.

To test the prediction of dielectrowetting induced spreading and reduction in contact angle, we initially used 1.29 μl volume droplets of 1, 2 propylene glycol deposited onto a 2 μm thick layer of SU-8 coating a set of parallel interdigitated electrodes of width 80 μm and gap of 80 μm fabricated on glass substrates (Fig. 1). To achieve a high ($\sim 90^\circ$) initial contact angle the SU-8 was treated with hydrophobising fluorocarbon solution. On applying a 10 kHz sinusoidal voltage of peak amplitude, V , rising from 0 V to 312 V the droplets of liquid increasingly spread along the direction of the electrodes with little or no spreading across the electrodes (Fig. 2). For an electrode width and gap between electrodes of, d , the electrical period is $4d$ giving a wave number $k=\pi/2d$. From Poisson's equation, the solution for the potential in a semi-infinite dielectric liquid is of the form $\sim \cos(kx)\exp(-kz)$, so that the penetration depth is related to the electrode structure by $\delta=4d/\pi$. Due to the periodicity of the electrodes and the energy barriers therefore introduced to motion across the electrodes, the liquid is expected to be confined to motion along the electrodes as observed in Fig. 2. Viewed perpendicular to the direction of spreading, the contact angle falls from 96° to 23° as the voltage is increased and then steadily increases back to 84° as the voltage is steadily diminished.

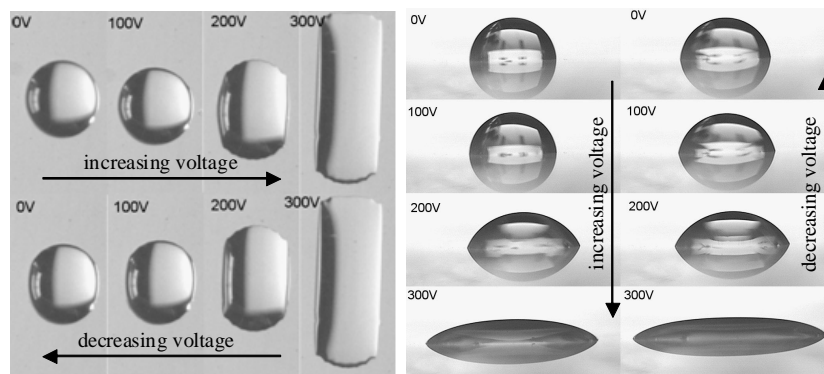


FIG. 2. Images of a 1, 2 propylene glycol droplet on a hydrophobic 2 μm thick SU-8 film on top of parallel planar interdigital electrodes of finger width and gap spacing of 80 μm : Views from above and in side-profile with camera aligned perpendicular to the electrodes as a 10 kHz peak-to-peak sinusoidal voltage is increased from 0 V to 312 V and back to 0V.

Figure 3 shows the quasistatic contact angle changes with applied voltage. The initial data point before the application of the voltage lies above the trend of the decreasing contact angle and this is due to it being above the receding contact angle for the surface. Similarly, the initial four data points as the voltage is reduced from its maximum lie away from the trend of the increasing contact angle due to the change from a receding contact angle to an advancing contact angle. In the regions where the contact angle decreases (or increases) steadily with voltage there is a linear dependence of $\cos\theta$ on V^2 as shown in the inset to Fig. 3. The increasing and decreasing voltage half-cycles are offset due to a small $\sim 6^\circ$ contact angle hysteresis. From this we concluded that L-DEP is able to spread droplets and that there is an initial regime, covering a very wide contact angle range ($\sim 70^\circ$), for which the functional form of equation (2) applies for this size of electrode structure and droplet volume.

Quantitatively, using the value $\epsilon_r=35.0$ for the relative permittivity of the oil and a value of $\gamma_{LV}=38 \text{ mN m}^{-1}$ for the surface tension so that $(\epsilon_r-1)/\gamma_{LV}=895 \text{ m N}^{-1}$, equation (2) predicts the slope of the data in Fig. 3 to be $m_p=0.39\times 10^{-4} \text{ V}^{-2}$. The experimentally observed value of $m_{exp}=1.07\times 10^{-4} \text{ V}^{-2}$ is of the same order of magnitude. To more accurately compare, we take into account that the SU-8 layer will cause a capacitive division of the voltage so that the effective voltage in the liquid,

V_c , is reduced compared to that applied to the interdigitated transducers, V_o . A simple model gives a voltage reduction factor, C , of,

$$C = \frac{\left(1 + \frac{\Delta\epsilon}{\epsilon}\right) e^{-2t_F/\delta}}{1 + \left(\frac{\Delta\epsilon}{\epsilon}\right) e^{-4t_F/\delta}} \quad (3)$$

where t_F is the thickness of the dielectric layer, $\Delta\epsilon/\epsilon = (\epsilon_F - \epsilon_{oil})/(\epsilon_F + \epsilon_{oil})$. For this experiment, using $\epsilon_{SU8}=3$ gives $C=0.685$ and the theoretical value of the slope is then $C^2 m_p = 0.83 \times 10^{-4} \text{ V}^{-2}$, which is 23% smaller than the experimentally observed value.

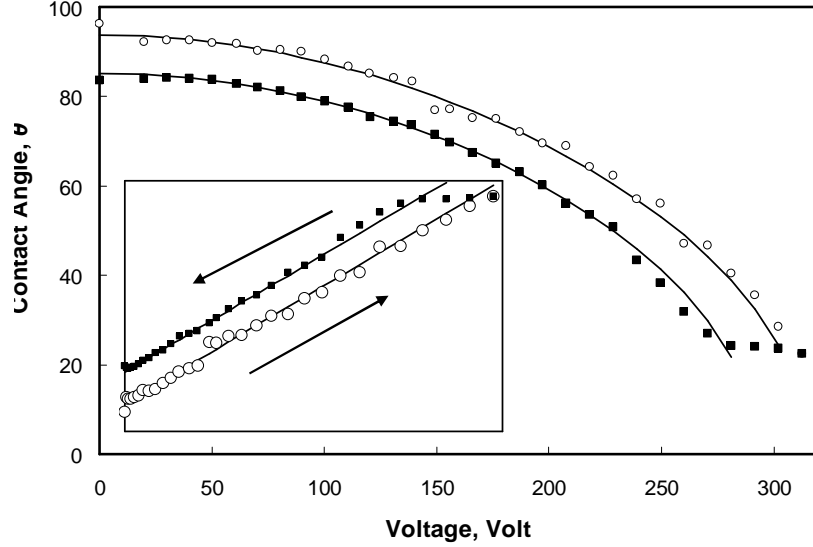


FIG. 3. The contact angle-voltage relationship for the data in fig. 1 (●●● symbols indicate the increasing voltage half cycle and ooo symbols indicate the decreasing voltage half cycle). The inset shows the data plotted as cosine contact angle versus voltage squared according to eq. (2); solid lines are fits to the linear regions using the average slope of the full data set. The hysteresis is caused by the switch from an advancing to a receding contact angle as the voltage changes from increasing to decreasing.

We repeated the initial experiments with interdigitated electrodes of reduced widths $20 \mu\text{m}$ and $40 \mu\text{m}$ (with gap sizes the same as electrode widths) capped with an SU-8 layer of $0.6 \mu\text{m}$, and in each case reversible voltage controlled spreading was observed. The functional form, $\cos\theta \propto V^2$ of equation (2) was found to fit the data for both increasing and decreasing voltages, although we did observe a slight systematic reduction of the slope on the reducing voltage half-cycles compared to the increasing voltage half-cycles as electrode size decreased to $20 \mu\text{m}$. To compare to the data for the $80 \mu\text{m}$ width electrodes, figure 4a shows the decreasing voltage half-cycle for $\cos\theta$ plotted against the ratio of effective voltage V_c^2 to the mechanical pitch $p=2d$ for the data in figure 3 with the data for the two other electrode sizes overlaid. In these cases, the reduction factors C from equation (3) which have been used are 0.613, 0.760 and 0.655 for the $20 \mu\text{m}$, $40 \mu\text{m}$ and $80 \mu\text{m}$ electrode widths, respectively, where a value $(\epsilon_F - 1)/\gamma_{LV} = 1057 \text{ m N}^{-1}$ for propylene glycol has been used to match the data in figure 3. Figure 4b shows $\cos\theta$ plotted against the effective voltage V_c^2 for the three electrode pitches; the solid lines are the individual lines of best fit. These data illustrate control of the strength of dielectrowetting by selection of the electrode pitch and, hence, scaling the penetration depth of the electric potential.

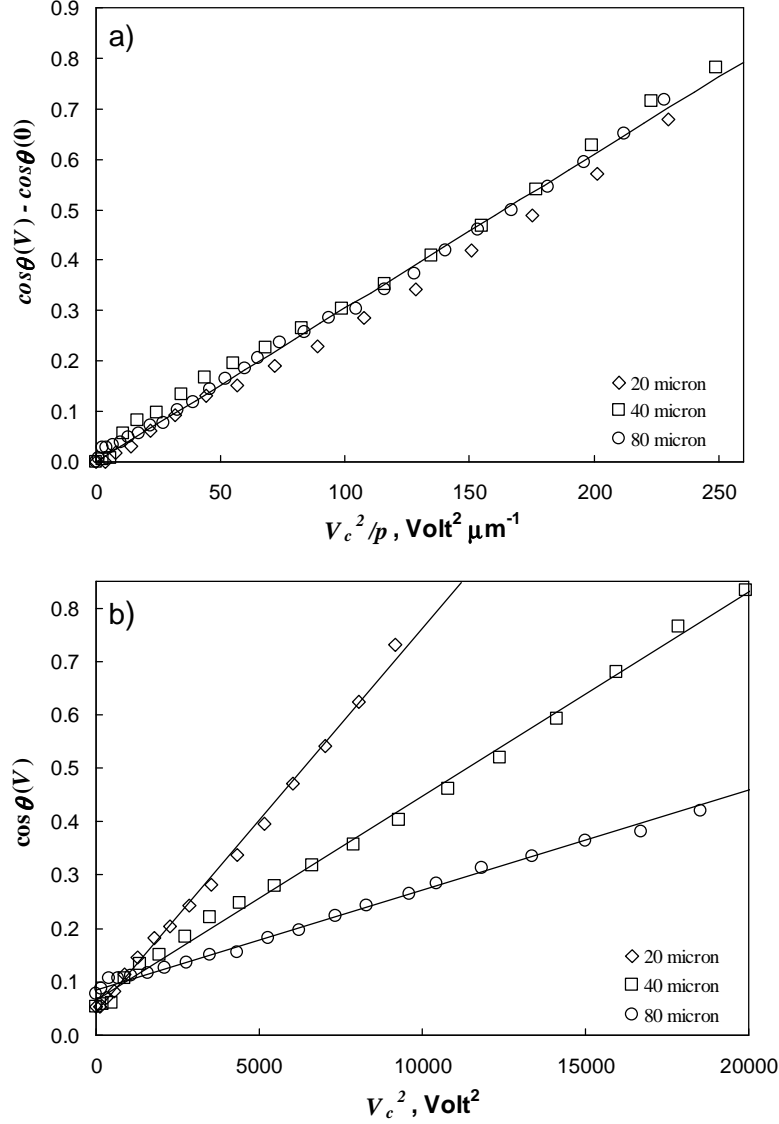


FIG. 4. (a) Data for three electrode pitches (20, 40 and 80 μm) plotted as a function of the effective voltage normalized by electrode mechanical pitch. The effective voltage takes into account the capacitive division caused by the solid dielectric layer on the interdigitated electrodes. (b) Data presented showing the effect of reducing the electric potential penetration depth into the liquid caused by changing the electrode mechanical pitch.

In this work, we have focused on droplets which have a thickness greater than the penetration depth set by the non-uniform electric field generated by an interdigitated electrode structure. At these droplet thickness to penetration depth ratios there is little possibility of the liquid-vapor interface beyond the penetration depth deforming to minimize the droplet surface free energy. However, as a droplet becomes thinner and more of a thin liquid film this assumption will break down and the liquid-vapor interface will wrinkle to adjust the overall energy balance between dielectrophoresis and surface free energies. For a planar parallel set of interdigital transducers the free surface of the liquid then first takes on a sinusoidal wrinkled appearance followed by a more complex non-sinusoidal wrinkle reflecting the concentration of electric field gradients at the electrode edges.²³ Here, our studies have also focused on non-aqueous liquids lacking free ionic charges and in air, but may also be relevant to reports of contact-less EWOD.²⁴ Furthermore,

electric fields can penetrate salt solutions typically used in electrowetting despite their DC electrical conductivity when they are applied with a sufficiently high frequency.²⁵ It should therefore be possible to control droplet contact angle for a full range of liquids simply by choosing a suitably high frequency of applied voltage. This also means that two-liquid systems rather than a liquid droplet in air, necessary for applications such as liquid-optics requiring neutral buoyancy, will be possible.

In summary, our approach shows how liquid dielectrophoresis can be used as an effect to reduce the contact angle of a droplet in a voltage controlled manner. This dielectrowetting effect is complementary to electrowetting, is based upon inhomogeneous electrostatic fields and does not require the liquid to be conducting or to be contacted by the electrodes. Our observations show that provided the droplet has a thickness larger than the penetration depth of the electric potential the cosine of the contact angle has a simple square law dependence on the applied voltage. The ability to control the contact angle by dielectrowetting has significance for processes such as droplet-based microfluidics, lab-on-a-chip systems, liquid-based optics, coating and other processes where enhanced or controlled spreading are desired. Finally, it is possible that dielectrowetting can be combined with superoleophobicity to create control of non-aqueous droplets across the full contact angle range.

References

- [1]. D. Quéré, *Ann. Rev. Mater. Res.* **38**, 71 (2008).
- [2]. N. J. Shirtcliffe, G. McHale, S. Atherton and M. I. Newton, *Adv. Colloid Interf. Sci.* **161**, 124 (2010).
- [3]. F. Mugele and J. C. Baret, *J. Phys.: Condens. Matt.* **17**, R705 (2005).
- [4]. T. M. Squires and S. R. Quake, *Rev. Mod. Phys.* **77**, 977 (2005).
- [5]. J. Heikenfeld, K. Zhou, E. Kreit, B. Raj, S. Yang, B. Sun, A. Milarcik, L. Clapp and R. Schwartz, *Nature Photonics* **3**, 292 (2009).
- [6]. C. V. Brown, G. G. Wells, M. I. Newton and G. McHale, *Nature Photonics* **3**, 403 (2009).
- [7]. M. Vallet, B. Berge and L. Vovelle, *Polymer* **37**, 2465 (1996).
- [8]. B. Berge, *Comptes Rendus de l' Academie des Sciences Serie II* **317**, 157 (1993).
- [9]. D. Mark, S. Haerberle, G. Roth, F. von Stetten and R. Zengerle, *Chem. Soc. Rev.* **39**, 1153 (2010).
- [10]. G. Pollack, R. B. Fair and A. D. Shenderov, *Appl. Phys. Lett.* **77**, 1725 (2000).
- [11]. R. B. Fair, *Microfluid. Nanofluid.* **3**, 245 (2007).
- [12]. R. A. Hayes and B. J. Feenstra, *Nature* **425**, 383 (2003).
- [13]. B. Berge and J. Peseux, *Eur. Phys. J.* **E3**, 159 (2000).
- [14]. S. Kuiper and B. H. W. Hendriks, *Appl. Phys. Lett.* **85**, 1128 (2004).
- [15]. T. N. Krupenkin, J. A. Taylor, T. M. Schneider and S. Yang, *Langmuir* **20**, 3824 (2004).
- [16]. T. D. Blake, A. Clarke and E. H. Stattersfield, *Langmuir* **16**, 2928 (2000).
- [17]. F. Li and F. Mugele, *Appl. Phys. Lett.* **92**, art. 244108 (2008).
- [18]. T. B. Jones, *Langmuir* **18**, 4437 (2002).
- [19]. T. B. Jones, M. Gunji, M. Washizu and M. J. Feldman, *J. Appl. Phys.* **89**, 1441 (2001).
- [20]. C.-C. Cheng, C. A. Chang, and J. A. Yeh, *Optics Express* **14**, 4101-6 (2006).
- [21]. Y.-C. Wang, Y.-C. Tsai, W.-P. Shih, *Microelectron. Engn.* **88**, 2748-2750 (2011).
- [22]. P. G. de Gennes, *Rev. Mod. Phys.* **57**, 827 (1985).
- [23]. C. V. Brown, W. Al-Shabib, G. G. Wells, G. McHale and M. I. Newton, *Appl. Phys. Lett.* **97**, art. 242904 (2010).
- [24]. A. G. Banpurkar, K. P. Nichols and F. Mugele, *Langmuir* **24**, 10549-10551 (2008).
- [25]. T. B. Jones and K. L. Wang, *Langmuir* **20**, 2813 (2004).

Acknowledgement

The authors' acknowledge the financial support of the UK EPSRC.